Predicting changes in neutralizing antibody activity for SARS-CoV-2 XBB.1.5 using *in silico* protein modeling

Colby T. Ford[1,2,✉], Shirish Yasa[3], Denis Jacob Machado[3,4], Richard Allen White III[3,4,5], and Daniel Janies[3,4]

[1]Tuple, LLC, Charlotte, NC, USA
[2]School of Data Science, University of North Carolina at Charlotte, Charlotte, NC, USA
[3]Dept. of Bioinformatics and Genomics, University of North Carolina at Charlotte, Charlotte, NC, USA
[4]Center for Computational Intelligence to Predict Health Environmental Risks (CIPHER), University of North Carolina at Charlotte, Charlotte, NC, USA
[5]North Carolina Research Campus (NCRC), University of North Carolina at Charlotte, Kannapolis, NC

The SARS-CoV-2 variant XBB.1.5 is of concern as it has high transmissibility. XBB.1.5 currently accounts for upwards of 30% of new infections in the United States. One year after our group published the predicted structure of the Omicron (B.1.1.529) variant's receptor binding domain (RBD) and antibody binding affinity, we return to investigate the new mutations seen in XBB.1.5 which is a descendant of Omicron. Using *in silico* modeling approaches against newer neutralizing antibodies that are shown effective against B.1.1.529, we predict the immune consequences of XBB.1.5's mutations and show that there is no statistically significant difference in overall antibody evasion when comparing to the B.1.1.529 and other related variants (e.g., BJ.1 and BM.1.1.1). However, noticeable changes in antibody binding affinity were seen due to specific amino acid changes of interest in the newer variants.

SARS-CoV-2 | Bioinformatics | Structure Prediction | Antibody Docking | SARS-CoV-2 variation

Correspondence: *colby.ford@uncc.edu or colby@tuple.xyz*

Introduction

In late November 2022, the United States Centers for Diseases Control stated that they began tracking a new SARS-CoV-2 variant known as XBB.1.5. At that time, XBB.1.5 was responsible for around 3% of all infections. Since then, XBB.1.5 has grown to represent 30% of all infections by January 2023 (1, 2).

XBB.1.5 is characterized by 40 mutations in the Spike protein, 22 of which are in the receptor binding domain (RBD) (3). The highly prevalent mutations in the RBD are shown in Table 1 below.

A health concern is that XBB.1.5 may evade existing antibodies derived from therapeutics, vaccination, and or previous Omicron (B.1.1.529) infection. It has been proposed that XBB.1.5 is a recombinant strain of the virus from BJ.1 and BM.1.1.1 as portions of the mutated Spike protein appear to be from each parent strain (4, 5). However, alternative hypotheses such as convergent evolution may also explain the similarity of portions of XBB.1.5's mutated regions to those seen in other variants (6, 7).

In our previous work on the prediction of the receptor binding domain (RBD) structure of the Omicron variant, our process provided robust predictions, having a root mean square de-

Mutation	Sequences	Prevalence
G339H	10,000	98.35%
R346T	9,992	98.27%
L368I	9,839	96.76%
S371F	9,857	96.94%
S373P	9,856	96.93%
S375F	9,860	96.97%
T376A	9,852	96.89%
D405N	9,895	97.32%
R408S	9,616	94.57%
K417N	9,329	91.75%
N440K	9,687	95.27%
V445P	9,653	94.94%
G446S	9,673	95.13%
N460K	9,757	95.96%
S477N	9,984	98.19%
T478K	9,960	97.95%
E484A	9,943	97.79%
F486P	9,919	97.55%
F490S	9,927	97.63%
Q498R	9,970	98.05%
N501Y	9,983	98.18%
Y505H	9,969	98.04%

Table 1. Prevalence of mutations in receptor binding domain of XBB.1.5. Prevalence is calculated as the percentage of samples (out of 10,168 from GISAID captured on February 12, 2023) that contain that mutation. Positions are numbered as their location in the larger Spike protein. These mutations are in comparison to the NC_045512.2 reference genome.

viation of atomic positions (RMSD) of 0.574Å between the predicted and empirically derived Omicron RBD structure (PDB: 7t9j) (8). Furthermore, our previous study proved useful as a predictive gauge of antibody efficacy several weeks prior to when empirical validations of the Omicron-antibody binding changes could be performed (9).

In this study, we use the methodology in our previous work to investigate XBB.1.5 and related variants (B.1.1.529, BJ.1, and BM.1.1) and expand the antibodies of interest to include more recently developed anti-Omicron antibodies. At the molecular level, we further elucidate the antibody binding and interfacing residues between three commercially-available antibodies: bamlanivimab, bebtelovimab, and tixagevimab and the RBD structure of each SARS-CoV-2 variant. We consider *in vitro* studies with existing antibodies and older variants to predict performance on XBB.1.5.

Results

Given the four SARS-CoV-2 variants (B.1.1.529, BJ.1, BM.1.1, and XBB.1.5) and 10 antibodies, 40 *in silico* docking experiments were performed. As shown in Figure 1, the mean performance of the included neutralizing antibodies is similar across the four variants, with XBB.1.5 binding results being congruent to that of B.1.1.529. Furthermore, across the 10 antibodies tested, the binding affinities seen in XBB.1.5 are not weakened compared to B.1.1.529, nor are the differences statistically significant.

When assessing overall antibody performance against BJ.1, we see weakened Van der Waals energies as compared to the other three variants. This is depicted in the Uniform Manifold Approximation and Projection (UMAP) in Figure 2 where the position of some antibodies on the BJ.1 UMAP are increased (leading to decreased binding affinity). However, desolvation energies and the buried surface areas are slightly improved overall when comparing BJ.1 results to the other three variant results.
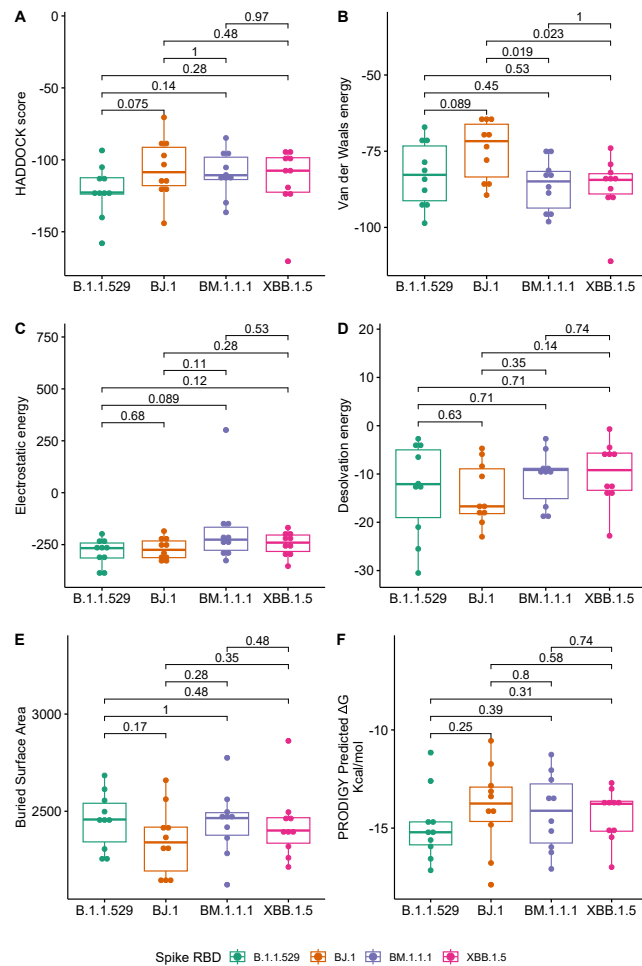

Fig. 1. Boxplots of antibody binding performance by SARS-CoV-2 variant. Wilcoxon *p*-values are shown to assess the statistical significance of the differences between overall variant-antibody performance.

While there are instances of overall antibody performance increasing or decreasing in singular comparisons, we do not see an overarching pattern that indicates that XBB.1.5

has evolved antibody evasion over B.1.1.529 (or BJ.1 and BM.1.1.1). In other words, XBB.1.5 does not appear to have evolved past current antibody defenses, specifically concerning the ten antibody structures tested in this study.
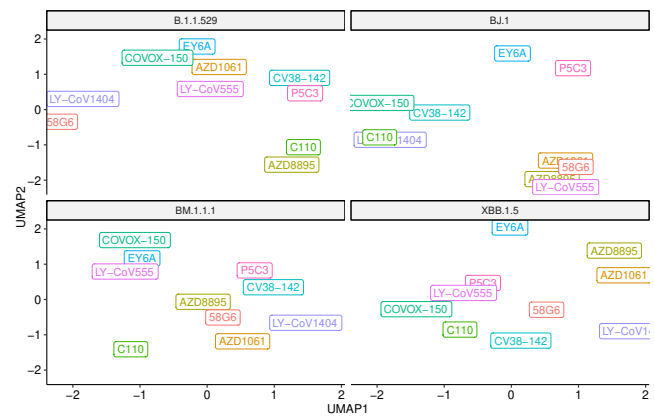

Fig. 2. UMAP scatter plot of antibody binding affinity metrics with a variant in each quadrant. Note that a higher UMAP value is likely indicative of worse performance.

Structural Changes in Antibody Binding Affinity. Of the ten antibodies tested in this study, we focus on the structural bases in which the antibodies LY-CoV555, LY-CoV1404, and AZD8895 work. The neutralization mechanisms of three antibodies have been extensively studied. These three antibodies have been available as therapeutics for treatment against COVID-19 infections (either currently or previously in the United States under Emergency Use Authorization) (10–12).

Bamlanivimab (LY-CoV555). As shown in Figure 3, we see a consistent interaction between Bamlanivimab (LY-CoV555) and the variant RBDs at R/Q493. This differs from Jones et al. (13), which states that F490 and S494 in the RBD are the interfacing residues in this region.
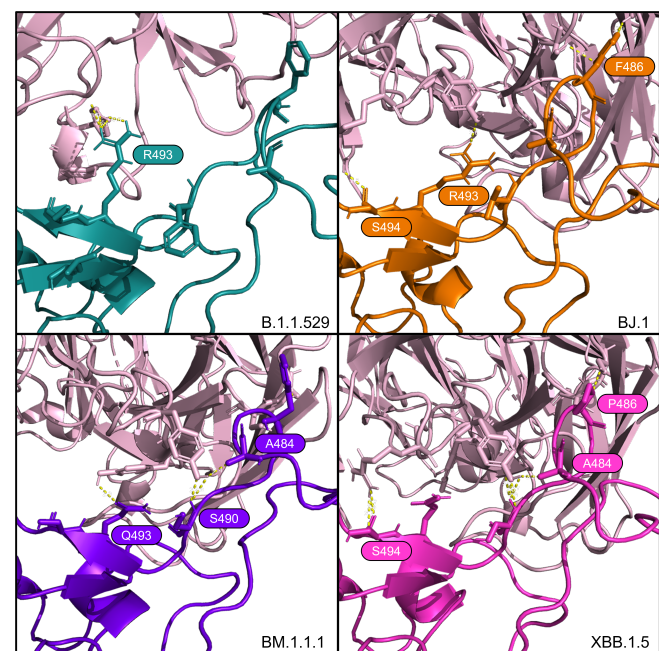

Fig. 3. Interfacing residues of interest from the LY-CoV555 antibody (in pale pink) against the four RBD structures.

The PyMOL structural visualizations of the potential interaction residues coincides with the overall metrics returned from the HADDOCK analyses shown in Table 2. LY-CoV555 shows the worst overall performance against BJ.1 while the performance against B.1.1.529, BM.1.1.1, and XBB.1.5 are quite similar. Though not shown in Figure 3, the latter three complexes show a higher number of interfacing residues overall than in BJ.1, thus supporting the reported affinity metrics.

Metric	B.1.1.529	BJ.1	BM.1.1.1	XBB.1.5
HADDOCK score	-105.1±8.4	-70.5±10.7	-105.3±3.1	-93.4±8.7
Van der Waals energy	-87.8±5.1	-65.1±6.2	-95.3±6.1	-87.3±2.6
Electrostatic energy	-237.1±14.3	-184.9±39.4	-148.7±14.1	-168.2±18.7
Desolvation energy	-12±1.2	-17.1±5.2	-18.7±3.6	-13±3
Buried Surface Area	2498.1±63.6	2155.5±97.3	2462.9±68.0	2386±52.3
Average ΔG (σ)	-14.78 (0.13)	-14.16 (0.26)	-14.59 (1.15)	-14.21 (0.86)

Table 2. Docking metrics for the LY-CoV555 antibody against the four RBD variants.

Bebtelovimab (LY-CoV1404). Westendorf et al. (14) demonstrated that Bebtelovimab (LY-CoV1404) antibody binding affinity may not be affected by RBD mutations at E484, F490, Q493. Shown in Figure 4, we see consistent interactions from this antibody across all four variants around most of these positions in spite of mutations.
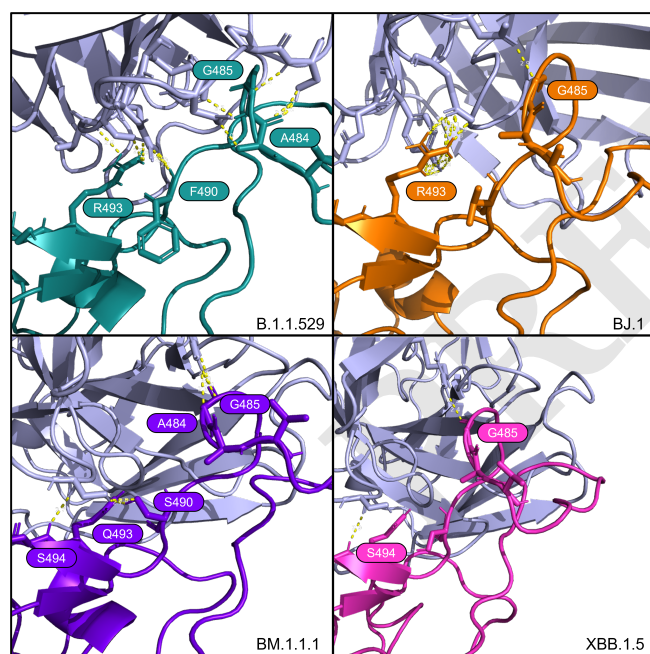

Fig. 4. Interfacing residues of interest from the LY-CoV1404 antibody (in light purple) against the four RBD structures.

These findings for LY-CoV1404 are congruent with the reported affinity metrics from the HADDOCK analyses shown in Table 3. Overall, HADDOCK scores are stable across the four variant complexes. The antibody LY-CoV1494 is predicted to have a slightly weaker interaction with XBB.1.5 compared to the other three variants.

Metric	B.1.1.529	BJ.1	BM.1.1.1	XBB.1.5
HADDOCK score	-124±1.1	-115.4±1.8	-110.9±6.3	-109.1±8.5
Van der Waals energy	-78.6±10.8	-63.9±4.7	-75.8±5.4	-74±3.0
Electrostatic energy	-262.1±24.3	-337.7±27.6	-290.7±16.1	-291.8±7.3
Desolvation energy	-30.5±7.1	-23±6.2	-2.7±2.8	-4.5±3.5
Buried Surface Area	2457.2±111.6	2365.5±71.9	2467.1±80.9	2454.9±65.1
Average ΔG (σ)	-16.47 (0.78)	-12.65 (0.53)	-19.90 (0.59)	-13.54 (0.88)

Table 3. Docking metrics for the LY-CoV1404 antibody against the four RBD variants.

Tixagevimab (AZD8895). For tixagevimab (AZD8895), as reported in Dong et al. (15), there is a critical contact residue at F486 on the RBD. We see this residue being interfaced in B.1.1.529, BJ.1, and BM.1.1.1. However, the F486 residue is mutated to proline at this position in XBB.1.5, though interactions from the antibody to the adjacent RBD residues at G485 and N487 of the RBD still occur. See Figure 5.
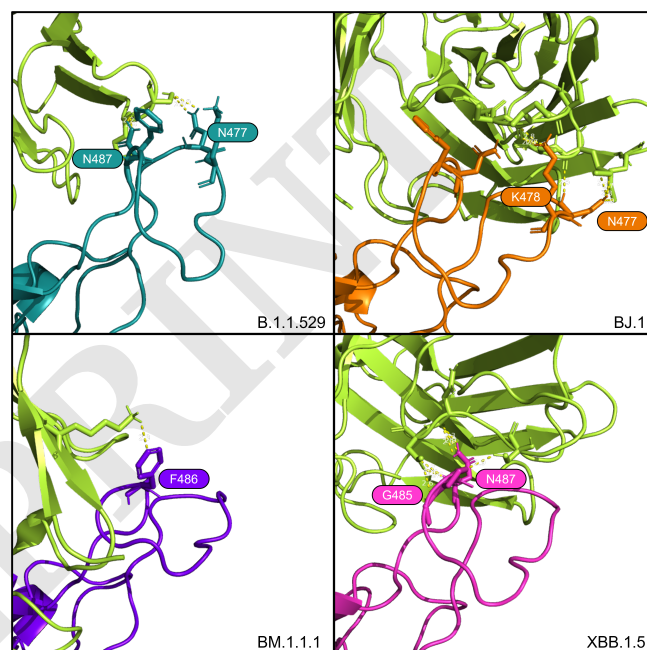

Fig. 5. Interfacing residues of interest from the AZD8895 antibody (in bright green) against the four RBD structures.

From the HADDOCK metrics shown in Table 4, this F486P mutation increases the binding affinity with the AZD8895, especially in terms of Van der Waals and electrostatic energies. Interfacing residues are abundant across all four of these AZD8895-RBD complexes (in addition to those shown in Figure 5), thus providing additional agreement to the strong affinity metrics reported by HADDOCK.

Metric	B.1.1.529	BJ.1	BM.1.1.1	XBB.1.5
HADDOCK score	-93.5±4.3	-88±6.7	-84.8±3.2	-123.8±6.9
Van der Waals energy	-71.5±6.6	-64.3±5.5	-86.7±3	-90.7±4.4
Electrostatic energy	-230±29.9	-215.5±5.9	-150±11.3	-256.3±222.6
Desolvation energy	-4.5±1.5	-8.4±5.7	-8.9±1.6	-5.5±2.8
Buried Surface Area	2259.5±49.1	2134.6±116.6	2482±46.4	2470.8±53.5
Average ΔG (σ)	-12.55 (0.21)	-11.76 (1.78)	-13.08 (0.36)	-13.01 (0.77)

Table 4. Docking metrics for the AZD8895 antibody against the four RBD variants.

Methods

Our *in silico* modeling approach includes the curation or generation of the RBD structures for four SARS-CoV-2 variants and ten neutralizing antibody structures. Next, each antibody structure was docked against each RBD structure and binding affinity metrics were collected for comparison.

RBD Structures. The Spike protein structure of the SARS-CoV-2 Omicron variant (B.1.1.529) was obtained from Protein Data Bank (PDB: 7t9j) (16). This structure was then trimmed to the RBD residues 339-528.

RBD sequences for BJ.1, BM.1.1.1, and XBB.1.5 were derived from representative samples found on GISAID:

<div align="center">

BJ.1: EPI_ISL_16182897
BM.1.1: EPI_ISL_15658180
XBB.1.5: EPI_ISL_16505393

</div>

The RBD structures of BJ.1, BM.1.1.1, and XBB.1.5 were predicted with these sequences using AlphaFold2 (ColabFold-mmseqs2 version) (17, 18). Next, the most confident structure of each was used in docking analyses.

Antibody Structures. Representative antibody structures were collected from various Protein Data Bank entries ranging from antibodies derived from infected patients (or patients with breakthrough infections) or commercially available antibodies used in the treatment of COVID-19. See Table 5.

Only a fragment antigen-binding (Fab) region of the antibodies was used in the docking analyses.

Antibody	Other Names	PDB ID	Citation
LY-CoV555	bamlanivimab, LY3819253	7kmg	Jones et al.
LY-CoV1404	bebtelovimab, LY3853113	7mmo	Westendorf et al.
AZD1061	cilgavimab	7l7e	Dong et al.
AZD8895	tixagevimab	7l7e	Dong et al.
58G6		7e3l	Li et al.
CV38-142		7lm9	Liu et al.
C110		7k8p	Barnes et al.
P5C3		7qtj	Fenwick et al.
EY6A		7zf3	Nutalai et al.
COVOX-150		7zf8	Nutalai et al.

Table 5. List of antibodies and their source PDB IDs used in this work.

Docking. To prepare the Fab structures, we renumbered residues according to HADDOCK's requirements such that there are no overlapping residue IDs between the heavy and light chains of the Fab's `.PDB` file. Residues in the Fab structures' complementarity-determining regions (CDRs) were selected as "active residues" for the docking analyses.

Residues in the S1 position of the RBD were selected as the "active residues" of the RBD structures. Since all of the input RBD `.PDB` files were renumbered to numbers 339-528, all of the input RBD files share the same "active residue" numbers. Each of the ten antibody structures where docked against each of the four RBD structures using HADDOCK v2.4, a biomolecular modeling software that provides docking predictions for provided structures (27).

The HADDOCK system outputs multiple metrics for the predicted binding affinities and an output set of `.PDB` files

containing the antibody docked against the RBD protein. PRODIGY, a tool to predict binding affinities using Gibbs energy, reported as ΔG in Kcal/mol units), was also run on each of the complexes (28).

This process resulted in forty sets of docked structures. Each set contains many antibody-RBD complex conformations, from which we selected the top-performing structure for each antibody-RBD pair. We used this top-performing complex for subsequent structural investigations into interfacing residues and docking positions.

These analyses were performed on the antibody-RBD structure pairs shown in Figure 1. The multiple metrics were used to assess the overall binding affinity changes between SARS-CoV-2 variants across multiple representative antibodies.

Further, the docked Protein Data bank Files (PDB) were manually reviewed using PyMOL (29) to search for interfacing residues and polar contacts between the RBD and Fab structures that may indicate neutralizing activity.

Conclusions

Building on our previous work (8) in studying Omicron's structure, we have continued to demonstrate the utility of *in silico* modeling for predicting whether antibody binding affinity changes with the evolution of new SARS-CoV-2 variants. Given that *in vitro* assessment of protein structure and antibody binding experiments are costly and take an extended time, *in silico* computational modeling provides a more economical and faster method near or at empirical resolution. Our previous *in silico* results were confirmed via an empirical study reported by VanBlargan et al. (9).

With computational modeling we rapidly preditct the potential severity of a new variant and provides predictions on antibody binding affinity. These predictions inform public health considerations and provide a method of rational drug design based on expected therapeutic and vaccine (and booster) efficacy. Computational modeling can be used to rapidly infer the public health consequences of a new variant in terms of the loss of efficacy of antibodies, such as breakthrough infections and associated healthcare burden.

For XBB.1.5 specifically, there are residue mutations of interest that may affect antibody binding of the various S1 region-binding antibodies tested here. Comparing previous reports on older variants concerning the three main antibodies discussed here to our computational results shows strong agreement between previous empirical results and our new *in silico* predictions.

For Bamlanivimab (LY-CoV555), Jones et al. (13) reported that mutations at RBD positions V483, E484, F490, and S494 either decrease or eliminate binding and function. Our study does not refute this, however, our computational modeling indicates the S494 is interfaced in the BJ.1 and XBB.1.5 interactions with LY-CoV555. This result suggests that this residue does not decrease the binding affinity of the antibody. Also, R/Q493 forms a polar interaction with LY-CoV555 in B.1.1.529, BJ.1, and BM.1.1.1, but not XBB.1.5.

In Bebtelovimab (LY-CoV1404), Westendorf et al. (14) states that mutations at E484 may confer advantages in antibody

evasion capabilities for the virus. This result is supported in our study as A484 in our four variants in this study, is only interfaced in our docked structures for B.1.1.529 and BM.1.1.1. We see G485 as an important interfacing residue, forming a polar contact with LY-CoV1404 with all four RBD variants.

Lastly, Dong et al. (15) reports that aromatic residues from AZD8895 CDR loops form a hydrophobic pocket with the RBD residues G485, F486, and N487. Note that in XBB.1.5 there is a F486P mutation and, interestingly, the adjacent residues (G485 and N487) are interfaced in our predicted complex. It is possible the proline at position 486 provides less steric hindrance than phenylalanine, thus allowing surrounding residue interaction. This result can be tested in future studies.

The increased binding affinity of XBB.1.5 for ACE2 may lead to increased transmissibility at the population level (30). The results here do not indicate that we can expect increased disease severity on an individual level for patients that avail themselves of therapeutics and vaccination.

The climb in cases of COVID-19 disease linked to XBB.1.5 indicates that XBB.1.5 could be a very serious subvariant of Omicron. While other studies are needed to assess transmissibility, virulence, pathogenicity, and other facets of viral severity and epidemiology, this study predicts that many current therapeutic and infection-derived antibodies provide antibody binding affinities similar to B.1.1.529 for XBB.1.5. Thus, the results indicate that the health care outcomes should be positive for the patients that avail themselves of vaccines and therapeutics.

Limitations and Future Work. This work estimates potential changes in antibody neutralization effects or antibody neutralizing affinity using *in silico* protein modeling and computational docking analyses. Given the computational and predictive nature of this study, empirical investigations are necessary to validate these findings. However, these computational approaches provide an economical, scalabl, and rapid methodology to understand the severity of new viral variants while the empirical work is being completed. Also, while HADDOCK is considered state-of-the-art in terms of protein docking, there are other docking tools that could pose different results for the comparisons

While we tested 10 representative neutralizing antibody structures against four variants of SARS-CoV-2, there are many more and antibody-variant RBD complexes to be assessed. In future work, we shall improve and automate our docking pipeline to enable to large-scale prediction of antibody binding affinity changes across any future SARS-CoV-2 variants of interest. Also, given the dynamic nature of protein structure conformations, alternative conformations may exist that show other polar contacts and antibody-RBD interfaces than those shown by the best performing HADDOCK complexes. All docking outputs and results, including those not shown in the body of this article, are available in the Supplementary Materials.

Supplementary Materials

All code, data, results, docking parameters, and protein structure files can be found on GitHub at https://github.com/colbyford/SARS-CoV-2_XBB.1.5_Spike-RBD_Predictions.

Conflict of Interest

Author CTF is the owner of Tuple, LLC. The remaining authors declare that the research was conducted in the absence of any commercial or financial relationships that could be construed as a potential conflict of interest.

Bibliography

1. Ewen Callaway. Coronavirus variant XBB.1.5 rises in the united states - is it a global threat? *Nature*, 613(7943):222–223, January 2023.
2. E Callaway. Is coronavirus variant XBB.1.5 a global threat? *Nature*, 613:222–223, 1 2023. doi: 10.1038/d41586-023-00014-3.
3. Outbreak.info SARS-COV-2 data explorer - XBB.1.5, 2023. https://outbreak.info/compare-lineages?pango=XBB.1.5&gene=S&threshold=75&nthresh=1&sub=false&dark=false.
4. Rajesh Karyakarte, Rashmita Das, Sonali Dudhate, Jeanne Agarasen, Praveena Pillai, Priyanka Chandankhede, Rutika Labshetwar, Yogita Gadiyal, Mansi Rajmane, Preeti Kulkarni, et al. Clinical characteristics and outcomes of laboratory-confirmed SARS-CoV-2 cases infected with Omicron subvariants and XBB recombinant variant. *MedRxiv*, pages 2023–01, 2023. doi: 10.1101/2023.01.05.23284211.
5. Ninaad Lasrado, Ai-ris Collier, Jessica Miller, Nicole Hachmann, Jinyan Liu, Michaela Sciacca, Cindy Wu, Trisha Anand, Esther Bondzie, Jana Fisher, et al. Waning immunity against XBB.1.5 following bivalent mrna boosters. *bioRxiv*, pages 2023–01, 2023. doi: 10.1101/2023.01.22.525079.
6. Jessica Miller, Nicole P. Hachmann, Ai-ris Y. Collier, Ninaad Lasrado, Camille R. Mazurek, Robert C. Patio, Olivia Powers, Nehalee Surve, James Theiler, Bette Korber, and Dan H. Barouch. Substantial Neutralization Escape by SARS-CoV-2 Omicron Variants BQ.1.1 and XBB.1. *New England Journal of Medicine*, 388(7):662–664, 2023. doi: 10.1056/NEJMc2214314. PMID: 36652339.
7. Yunlong Cao, Fanchong Jian, Jing Wang, Yuanling Yu, Weiliang Song, Ayijiang Yisimayi, Ran An, Xiaosu Chen, Na Zhang, Yao Wang, Peng Wang, Lijuan Zhao, Haiyan Sun, Lingling Yu, Sijie Yang, Xiao Niu, Tianhe Xiao, Qingqing Gu, Fei Shao, Xiaohua Hao, Yanli Xu, Ronghua Jin, Zhongyang Shen, Youchun Wang, and Xiaoliang Sunney Xie. Imprinted SARS-CoV-2 humoral immunity induces convergent Omicron RBD evolution. *Nature*, 614 (7948):521–529, Feb 2023. ISSN 1476-4687. doi: 10.1038/s41586-022-05644-7.
8. Colby T. Ford, Denis Jacob Machado, and Daniel A. Janies. Predictions of the SARS-CoV-2 Omicron Variant (B.1.1.529) Spike Protein Receptor-Binding Domain Structure and Neutralizing Antibody Interactions. *Frontiers in Virology*, 2, 2022. ISSN 2673-818X. doi: 10.3389/fviro.2022.830202.
9. Laura A. VanBlargan, John M. Errico, Peter J. Halfmann, Seth J. Zost, James E. Crowe, Lisa A. Purcell, Yoshihiro Kawaoka, Davide Corti, Daved H. Fremont, and Michael S. Diamond. An infectious sars-cov-2 b.1.1.529 omicron virus escapes neutralization by therapeutic monoclonal antibodies. *Nature Medicine*, 28(3):490–495, Mar 2022. ISSN 1546-170X. doi: 10.1038/s41591-021-01678-y.
10. US Food and Drug Administration. Emergency use authorization 094, 2022. https://pi.lilly.com/eua/bam-and-ete-eua-fda-authorization-letter.pdf.
11. US Food and Drug Administration. Emergency use authorization 111, 2022. https://www.fda.gov/media/156151/download.
12. US Food and Drug Administration. Emergency use authorization 104, 2023. https://www.fda.gov/media/154704/download.
13. Bryan E. Jones, Patricia L. Brown-Augsburger, Kizzmekia S. Corbett, Kathryn Westendorf, Julian Davies, Thomas P. Cujec, Christopher M. Wiethoff, Jamie L. Blackbourne, Beverly A. Heinz, Denisa Foster, Richard E. Higgs, Deepa Balasubramaniam, Lingshu Wang, Yi Zhang, Eun Sung Yang, Roza Bidshahri, Lucas Kraft, Yuri Hwang, Stefanie Žentelis, Kevin R. Jepson, Rodrigo Goya, Maia A. Smith, David W. Collins, Samuel J. Hinshaw, Sean A. Tycho, Davide Pellacani, Ping Xiang, Krithika Muthuraman, Solmaz Sobhanifar, Marissa H. Piper, Franz J. Triana, Jorg Hendle, Anna Pustilnik, Andrew C. Adams, Shawn J. Berens, Ralph S. Baric, David R. Martinez, Robert W. Cross, Thomas W. Geisbert, Viktoriya Borisevich, Olubukola Abiona, Hayley M. Belli, Maren de Vries, Adil Mohamed, Meike Dittmann, Marie I. Samanovic, Mark J. Mulligan, Jory A. Goldsmith, Ching-Lin Hsieh,

Nicole V. Johnson, Daniel Wrapp, Jason S. McLellan, Bryan C. Barnhart, Barney S. Graham, John R. Mascola, Carl L. Hansen, and Ester Falconer. The neutralizing antibody, ly-cov555, protects against sars-cov-2 infection in nonhuman primates. *Science Translational Medicine*, 13(593):eabf1906, 2021. doi: 10.1126/scitranslmed.abf1906.

14. Kathryn Westendorf, Stefanie Žentelis, Lingshu Wang, Denisa Foster, Peter Vaillancourt, Matthew Wiggin, Erica Lovett, Robin van der Lee, Jörg Hendle, Anna Pustilnik, J. Michael Sauder, Lucas Kraft, Yuri Hwang, Robert W. Siegel, Jinbiao Chen, Beverly A. Heinz, Richard E. Higgs, Nicole L. Kallewaard, Kevin Jepson, Rodrigo Goya, Maia A. Smith, David W. Collins, Davide Pellacani, Ping Xiang, Valentine de Puyraimond, Marketa Ricicova, Lindsay Devorkin, Caitlin Pritchard, Aoise O'Neill, Kush Dalal, Pankaj Panwar, Harveer Dhupar, Fabian A. Garces, Courtney A. Cohen, John M. Dye, Kathleen E. Huie, Catherine V. Badger, Darwyn Kobasa, Jonathan Audet, Joshua J. Freitas, Saleema Hassanali, Ina Hughes, Luis Munoz, Holly C. Palma, Bharathi Ramamurthy, Robert W. Cross, Thomas W. Geisbert, Vineet Menachery, Kumari Lokugamage, Viktoriya Borisevich, Iliana Lanz, Lisa Anderson, Payal Sipahimalani, Kizzmekia S. Corbett, Eun Sung Yang, Yi Zhang, Wei Shi, Tongqing Zhou, Misook Choe, John Misasi, Peter D. Kwong, Nancy J. Sullivan, Barney S. Graham, Tara L. Fernandez, Carl L. Hansen, Ester Falconer, John R. Mascola, Bryan E. Jones, and Bryan C. Barnhart. Ly-cov1404 (bebtelovimab) potently neutralizes sars-cov-2 variants. *Cell Reports*, 39(7):110812, 2022. ISSN 2211-1247. doi: https://doi.org/10.1016/j.celrep.2022.110812.

15. Jinhui Dong, Seth J. Zost, Allison J. Greaney, Tyler N. Starr, Adam S. Dingens, Elaine C. Chen, Rita E. Chen, James Brett Case, Rachel E. Sutton, Pavlo Gilchuk, Jessica Rodriguez, Erica Armstrong, Christopher Gainza, Rachel S. Nargi, Elad Binshtein, Xuping Xie, Xianwen Zhang, Pei-Yong Shi, James Logue, Stuart Weston, Marisa E. McGrath, Matthew B. Frieman, Tyler Brady, Kevin M. Tuffy, Helen Bright, Yueh-Ming Loo, Patrick M. McTamney, Mark T. Esser, Robert H. Carnahan, Michael S. Diamond, Jesse D. Bloom, and James E. Crowe. Genetic and structural basis for sars-cov-2 variant neutralization by a two-antibody cocktail. *Nature Microbiology*, 6(10):1233–1244, Oct 2021. ISSN 2058-5276. doi: 10.1038/s41564-021-00972-2.

16. Dhiraj Mannar, James W. Saville, Xing Zhu, Shanti S. Srivastava, Alison M. Berezuk, Katharine S. Tuttle, Ana Citlali Marquez, Inna Sekirov, and Sriram Subramaniam. SARS-CoV-2 Omicron variant: Antibody evasion and cryo-EM structure of spike protein-ACE2 complex. *Science*, 375(6582):760–764, 2022. doi: 10.1126/science.abn7760.

17. John Jumper, Richard Evans, Alexander Pritzel, Tim Green, Michael Figurnov, Olaf Ronneberger, Kathryn Tunyasuvunakool, Russ Bates, Augustin Žídek, Anna Potapenko, Alex Bridgland, Clemens Meyer, Simon A. A. Kohl, Andrew J. Ballard, Andrew Cowie, Bernardino Romera-Paredes, Stanislav Nikolov, Rishub Jain, Jonas Adler, Trevor Back, Stig Petersen, David Reiman, Ellen Clancy, Michal Zielinski, Martin Steinegger, Michalina Pacholska, Tamas Berghammer, Sebastian Bodenstein, David Silver, Oriol Vinyals, Andrew W. Senior, Koray Kavukcuoglu, Pushmeet Kohli, and Demis Hassabis. Highly accurate protein structure prediction with AlphaFold. *Nature*, 596(7873):583–589, Aug 2021. ISSN 1476-4687. doi: 10.1038/s41586-021-03819-2.

18. Milot Mirdita, Konstantin Schütze, Yoshitaka Moriwaki, Lim Heo, Sergey Ovchinnikov, and Martin Steinegger. ColabFold: making protein folding accessible to all. *Nature Methods*, 19 (6):679–682, Jun 2022. ISSN 1548-7105. doi: 10.1038/s41592-022-01488-1.

19. Bryan E. Jones, Patricia L. Brown-Augsburger, Kizzmekia S. Corbett, Kathryn Westendorf, Julian Davies, Thomas P. Cujec, Christopher M. Wiethoff, Jamie L. Blackbourne, Beverly A. Heinz, Denisa Foster, Richard E. Higgs, Deepa Balasubramaniam, Lingshu Wang, Yi Zhang, Eun Sung Yang, Roza Bidshahri, Lucas Kraft, Yuri Hwang, Stefanie Žentelis, Kevin R. Jepson, Rodrigo Goya, Maia A. Smith, David W. Collins, Samuel J. Hinshaw, Sean A. Tycho, Davide Pellacani, Ping Xiang, Krithika Muthuraman, Solmaz Sobhanifar, Marissa H. Piper, Franz J. Triana, Jorg Hendle, Anna Pustilnik, Andrew C. Adams, Shawn J. Berens, Ralph S. Baric, David R. Martinez, Robert W. Cross, Thomas W. Geisbert, Viktoriya Borisevich, Olubukola Abiona, Hayley M. Belli, Maren de Vries, Adil Mohamed, Meike Dittmann, Marie I. Samanovic, Mark J. Mulligan, Jory A. Goldsmith, Ching-Lin Hsieh, Nicole V. Johnson, Daniel Wrapp, Jason S. McLellan, Bryan C. Barnhart, Barney S. Graham, John R. Mascola, Carl L. Hansen, and Ester Falconer. The neutralizing antibody, LY-CoV555, protects against SARS-CoV-2 infection in nonhuman primates. *Science Translational Medicine*, 13(593):eabf1906, 2021. doi: 10.1126/scitranslmed.abf1906.

20. Kathryn Westendorf, Stefanie Žentelis, Lingshu Wang, Denisa Foster, Peter Vaillancourt, Matthew Wiggin, Erica Lovett, Robin van der Lee, Jörg Hendle, Anna Pustilnik, J. Michael Sauder, Lucas Kraft, Yuri Hwang, Robert W. Siegel, Jinbiao Chen, Beverly A. Heinz, Richard E. Higgs, Nicole L. Kallewaard, Kevin Jepson, Rodrigo Goya, Maia A. Smith, David W. Collins, Davide Pellacani, Ping Xiang, Valentine de Puyraimond, Marketa Ricicova, Lindsay Devorkin, Caitlin Pritchard, Aoise O'Neill, Kush Dalal, Pankaj Panwar, Harveer Dhupar, Fabian A. Garces, Courtney A. Cohen, John M. Dye, Kathleen E. Huie, Catherine V. Badger, Darwyn Kobasa, Jonathan Audet, Joshua J. Freitas, Saleema Hassanali, Ina Hughes, Luis Munoz, Holly C. Palma, Bharathi Ramamurthy, Robert W. Cross, Thomas W. Geisbert, Vineet Menachery, Kumari Lokugamage, Viktoriya Borisevich, Iliana Lanz, Lisa Anderson, Payal Sipahimalani, Kizzmekia S. Corbett, Eun Sung Yang, Yi Zhang, Wei Shi, Tongqing Zhou, Misook Choe, John Misasi, Peter D. Kwong, Nancy J. Sullivan, Barney S. Graham, Tara L. Fernandez, Carl L. Hansen, Ester Falconer, John R. Mascola, Bryan E. Jones, and Bryan C. Barnhart. LY-CoV1404 (bebtelovimab) potently neutralizes SARS-CoV-2 variants. *Cell Reports*, 39(7), May 2022. ISSN 2211-1247. doi: 10.1016/j.celrep.2022.110812.

21. Jinhui Dong, Seth J. Zost, Allison J. Greaney, Tyler N. Starr, Adam S. Dingens, Elaine C. Chen, Rita E. Chen, James Brett Case, Rachel E. Sutton, Pavlo Gilchuk, Jessica Rodriguez, Erica Armstrong, Christopher Gainza, Rachel S. Nargi, Elad Binshtein, Xuping Xie, Xianwen Zhang, Pei-Yong Shi, James Logue, Stuart Weston, Marisa E. McGrath, Matthew B. Frieman, Tyler Brady, Kevin M. Tuffy, Helen Bright, Yueh-Ming Loo, Patrick M. McTamney, Mark T. Esser, Robert H. Carnahan, Michael S. Diamond, Jesse D. Bloom, and James E. Crowe. Genetic and structural basis for SARS-CoV-2 variant neutralization by a two-antibody cocktail. *Nature Microbiology*, 6(10):1233–1244, Oct 2021. ISSN 2058-5276. doi: 10.1038/s41564-021-00972-2.

22. Tingting Li, Xiaojian Han, Chenjian Gu, Hangtian Guo, Huajun Zhang, Yingming Wang, Chao Hu, Kai Wang, Fengjiang Liu, Feiyang Luo, Yanan Zhang, Jie Hu, Wang Wang, Shenglong Li, Yanan Hao, Meiying Shen, Jingjing Huang, Yingyi Long, Shuyi Song, Ruixin Wu, Song Mu, Qian Chen, Fengxia Gao, Jianwei Wang, Shunhua Long, Luo Li, Yang Wu, Yan Gao, Wei Xu, Xia Cai, Di Qu, Zherui Zhang, Hongqing Zhang, Na Li, Qingzhu Gao, Guiji Zhang, Changlong He, Wei Wang, Xiaoyun Ji, Ni Tang, Zhenghong Yuan, Youhua Xie, Haitao Yang, Bo Zhang, Ailong Huang, and Aishun Jin. Potent SARS-CoV-2 neutralizing antibodies with protective efficacy against newly emerged mutational variants. *Nature Communications*, 12(1):6304, Nov 2021. ISSN 2041-1723. doi: 10.1038/s41467-021-26539-7.

23. Hejun Liu, Meng Yuan, Deli Huang, Sandhya Bangaru, Fangzhu Zhao, Chang-Chun D. Lee, Linghang Peng, Shawn Barman, Xueyong Zhu, David Nemazee, Dennis R. Burton, Marit J. van Gils, Rogier W. Sanders, Hans-Christian Kornau, S. Momsen Reincke, Harald Prüss, Jakob Kreye, Nicholas C. Wu, Andrew B. Ward, and Ian A. Wilson. A combination of cross-neutralizing antibodies synergizes to prevent SARS-CoV-2 and SARS-CoV pseudovirus infection. *Cell Host & Microbe*, 29(5):806–818.e6, May 2021. ISSN 1931-3128. doi: 10.1016/j.chom.2021.04.005.

24. Christopher O. Barnes, Claudia A. Jette, Morgan E. Abernathy, Kim-Marie A. Dam, Shannon R. Esswein, Harry B. Gristick, Andrey G. Malyutin, Naima G. Sharaf, Kathryn E. Huey-Tubman, Yu E. Lee, Davide F. Robbiani, Michel C. Nussenzweig, Anthony P. West, and Pamela J. Bjorkman. SARS-CoV-2 neutralizing antibody structures inform therapeutic strategies. *Nature*, 588(7839):682–687, Dec 2020. ISSN 1476-4687. doi: 10.1038/s41586-020-2852-1.

25. Craig Fenwick, Priscilla Turelli, Dongchun Ni, Laurent Perez, Kelvin Lau, Cécile Herate, Romain Marlin, Erica Lana, Céline Pellaton, Charlène Raclot, Line Esteves-Leuenberger, Jérémy Campos, Alex Farina, Flurin Fiscalini, Nathalie Dereuddre-Bosquet, Francis Relouzat, Rana Abdelnabi, Caroline S. Foo, Johan Neyts, Pieter Leyssen, Yves Lévy, Florence Pojer, Henning Stahlberg, Roger LeGrand, Didier Trono, and Giuseppe Pantaleo. Patient-derived monoclonal antibody neutralizes SARS-CoV-2 Omicron variants and confers full protection in monkeys. *Nature Microbiology*, 7(9):1376–1389, Sep 2022. ISSN 2058-5276. doi: 10.1038/s41564-022-01198-6.

26. Rungtiwa Nutalai, Daming Zhou, Aekkachai Tuekprakhon, Helen M. Ginn, Piyada Supasa, Chang Liu, Jiandong Huo, Alexander J. Mentzer, Helen M.E. Duyvesteyn, Aiste Dijokaite-Guraliuc, Donal Skelly, Thomas G. Ritter, Ali Amini, Sagida Bibi, Sandra Adele, Sile Ann Johnson, Bede Constantinides, Hermione Webster, Nigel Temperton, Paul Klenerman, Eleanor Barnes, Susanna J. Dunachie, Derrick Crook, Andrew J. Pollard, Teresa Lambe, Philip Goulder, Neil G. Paterson, Mark A. Williams, David R. Hall, Juthathip Mongkolsapaya, Elizabeth E. Fry, Wanwisa Dejnirattisai, Jingshan Ren, David I. Stuart, and Gavin R. Screaton. Potent cross-reactive antibodies following Omicron breakthrough in vaccinees. *Cell*, 185(12):2116–2131.e18, Jun 2022. ISSN 0092-8674. doi: 10.1016/j.cell.2022.05.014.

27. G.C.P. van Zundert, J.P.G.L.M. Rodrigues, M. Trellet, C. Schmitz, P.L. Kastritis, E. Karaca, A.S.J. Melquiond, M. van Dijk, S.J. de Vries, and A.M.J.J. Bonvin. The HADDOCK2.2 web server: User-friendly integrative modeling of biomolecular complexes. *Journal of Molecular Biology*, 428(4):720–725, 2016. doi: 10.1016/j.jmb.2015.09.014.

28. Anna Vangone and Alexandre MJJ Bonvin. Contacts-based prediction of binding affinity in protein–protein complexes. *eLife*, 4:e07454, jul 2015. ISSN 2050-084X. doi: 10.7554/eLife.07454.

29. Schrödinger, LLC. The PyMOL molecular graphics system, version 1.8. November 2015.

30. Can Yue, Weiliang Song, Lei Wang, Fanchong Jian, Xiaosu Chen, Fei Gao, Zhongyang Shen, Youchun Wang, Xiangxi Wang, and Yunlong Cao. ACE2 binding and antibody evasion in enhanced transmissibility of XBB.1.5. *The Lancet Infectious Diseases*, 2023/02/22 2023. ISSN 1473-3099. doi: 10.1016/S1473-3099(23)00010-5.

31. Sjoerd J. de Vries and Alexandre M. J. J. Bonvin. Cport: A consensus interface predictor and its performance in prediction-driven docking with haddock. *PLOS ONE*, 6(3):1–12, 03 2011. doi: 10.1371/journal.pone.0017695.

Supplementary Note 1: RBD Structural Alignment and Comparison

Using PyMOL's alignment tool (with 50 cycles and a cutoff of 2.0Å)(29), we superimposed the RBD structures as shown in Figure 6 and show RMSD metrics in Table 6.

Fig. 6. Cartoon representation of the four RBD structures aligned. B.1.1.529 (PDB: 7t9j) in teal, BJ.1 in orange, B.1.1.1 in purple, and XBB.1.5 in magenta with mutated residues from Table 1 highlighted in yellow.

Variant	B.1.1.529	BJ.1	BM.1.1.1	XBB.1.5
B.1.1.529	0	0.780	0.708	0.653
BJ.1	0.780	0	0.306	0.266
BM.1.1.1	0.708	0.306	0	0.146
XBB.1.5	0.653	0.266	0.146	0

Table 6. Alignment RMSD distance (in Ångstroms) between each variant's RBD structure.

Note that none of the mutations are predicted to disrupt the overall RBD tertiary structure in the AlphaFold2-generated structures. There are minor secondary structure changes as to where alpha helices or the anti-parallel beta sheet may begin or end, but overall the structures are very similar.

Looking at the main loop structure at the top of the S1 region, shown in Figure 7, the residue side chains are in similar positions, differing only by slight angular changes with the exception of the F486P mutation as previously mentioned. This proline mutation does not change the overall loop's conformation, but provides rigidity at this location.
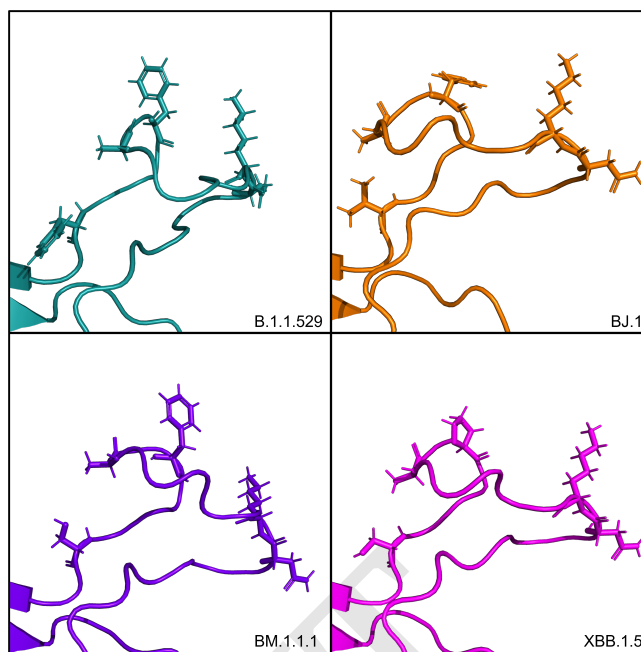

Fig. 7. Side chains of the main loop at the S1 binding site for each of four RBD structures. Residues that are mutated from the wild type reference are shown as sticks.

Supplementary Note 2: RBD Active Residue Predictions

Using CPORT, an interface predictor that provides a prediction of active and passive residues on a given protein (31), we evaluated the four RBD structures. This tool predicted that . See Table 7 below.

Variant	Active Residues	Passive Residues
B.1.1.529	357, 359, 360, 361, 390, 391, 394, 417, 452, 453, 455, 456, 457, 470, 471, 476, 478, 479, 481, 482, 483, 484, 485, 486, 487, 489, 490, 492, 493	338, 351, 352, 355, 356, 362, 382, 383, 386, 388, 389, 396, 403, 409, 415, 416, 420, 421, 449, 450, 458, 459, 460, 461, 462, 465, 467, 468, 469, 472, 473, 474, 475, 477, 480, 494, 515, 516, 517, 518, 520, 521, 522, 523, 525, 526, 527, 528
BJ.1	449, 450, 452, 455, 456, 457, 458, 459, 460, 461, 468, 469, 470, 471, 473, 474, 475, 476, 477, 478, 483, 484, 485, 486, 487, 489, 490, 493, 494	345, 346, 347, 351, 352, 403, 417, 419, 420, 421, 422, 444, 447, 448, 453, 462, 463, 465, 466, 467, 472, 479, 480, 481, 482, 495, 496, 497
BM.1.1.1	338, 339, 357, 359, 360, 361, 362, 363, 364, 367, 388, 391, 392, 393, 394, 452, 455, 456, 472, 475, 483, 484, 485, 486, 487, 489, 490, 493, 494	340, 343, 344, 349, 351, 352, 355, 356, 366, 369, 370, 371, 372, 374, 382, 383, 384, 385, 386, 389, 390, 396, 403, 417, 421, 430, 448, 450, 457, 458, 459, 469, 470, 471, 473, 474, 476, 477, 478, 479, 480, 481, 482, 492, 495, 496, 497, 515, 516, 517, 518, 519, 523, 524, 525, 526, 527, 528
XBB.1.5	351, 357, 358, 359, 360, 361, 390, 391, 393, 417, 421, 455, 456, 457, 483, 484, 485, 486, 487, 489, 493, 516, 518, 519, 520, 521, 522, 523, 525	338, 348, 352, 355, 356, 362, 364, 382, 383, 386, 388, 389, 396, 403, 409, 415, 416, 419, 420, 422, 430, 450, 452, 458, 459, 460, 461, 462, 465, 466, 467, 468, 469, 470, 471, 472, 473, 474, 475, 480, 490, 492, 514, 515, 517, 527, 528

Table 7. CPORT-predicted active and passive residues of the four RBD structures.

Also, if we look at the residues that were predicted to be active visually, we can see that the majority of these residues concentrate around the S1 area of the RBD. Specifically, the loop structure on the top of the RBD that has been discussed

heavily in this study and previous works is consistently predicted to contain multiple active residues across all four variant structures. See Figure 8.
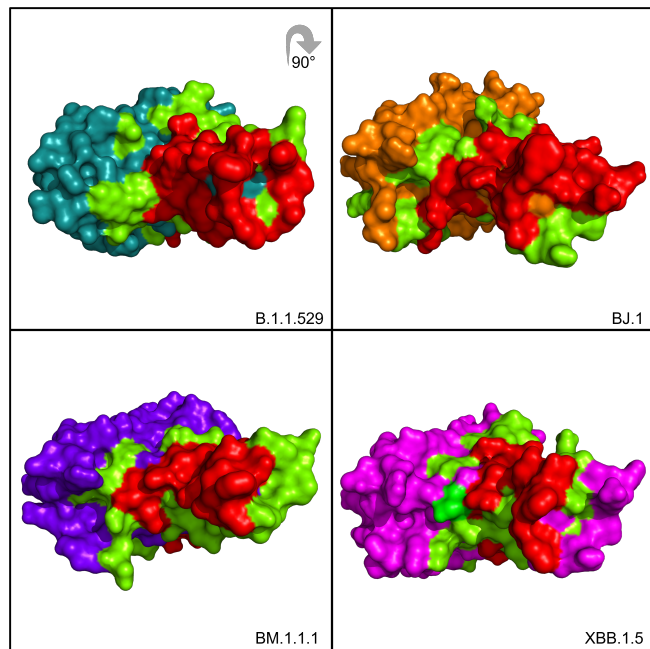

Fig. 8. CPORT predicted active and passive residues (in red and green, respectively) of the four RBD structures. Shown as the "top" of the RBD, 90° foward.

There is considerable agreement between the CPORT predictions and the HADDOCK results listed in the main article. Nearly all of the interfacing residues detected in the complexes shown in Figures 3, 4, and 5 are predicted to be active residues from CPORT. Furthermore, many of these predicted active residues are also mentioned in Jones et al. (13), Westendorf et al. (14) and Dong et al. (15), thus further supporting that these residues on the top of the S1 region stand as the likely epitope between the RBD and various neutralizing antibodies evaluated in this study.

Supplementary Note 3: PRODIGY Results

In Figure 1, we show the top performing antibody-RBD complexes' HADDOCK and PRODIGY scores. That is, the metrics for the top performing complex from the top performing HADDOCK cluster. In Figure 9 below, we show the individual PRODIGY scores of the top four complexes from the top performing HADDOCK cluster for each antibody-RBD experiment. There is agreement that no statistically significant drop in overall antibody binding affinity in terms of ΔG as predicted by PRODIGY.
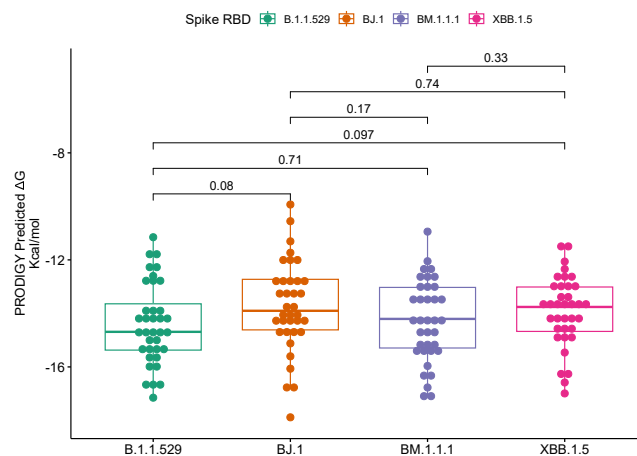

Fig. 9. PRODIGY binding affinity metrics for the top four clusters in each antibody-RBD complex that resulted from the HADDOCK docking process.

Ford *et al.* | Is XBB.1.5 evading neutralizing antibodies?